

# Nonlinear Optical Properties of Poly-*p*-(phenylene terephthalates) with Side Group Chromophores

Suck-Hyun Lee,<sup>\*,†</sup> Yong-Ki Kim,<sup>‡</sup> and Young-Hee Won<sup>‡</sup>

Departments of Applied Chemistry and Physics, Ajou University, Suwon, Korea 441-749

Received May 11, 1998; Revised Manuscript Received September 28, 1998

**ABSTRACT:** The linear and nonlinear optical (NLO) properties are reported for a series of wholly aromatic polyesters containing NLO chromophores in the side group through a different alkyl tether length. For the first time, we have observed the domain structures of NLO chromophores for the poled thin-film samples of the polymers using atomic force microscopy. Measurements on the refractive indices of the transverse magnetic and transverse electric modes exhibited considerable anisotropy for the films as spin-coated and poled. The measured positive birefringences were greater for the polymer with shorter tether length, indicating a more pronounced orientation of the optically anisotropic groups in the direction of the film plane. SHG measurements also showed that small changes in the number of methylene units in the side spacer result in large changes in the second-order NLO properties. The tensor ratios of the NLO components were revealed to be smaller than  $d_{33}/d_{31} = 3$ , the predicted value by the isotropic model for a purely electronic response. This behavior was understood in terms of the different orientations of the chromophore through the sample thickness, that is, a surface domain layer with normal orientation and a compressed inner layer with tilted orientation.

## Introduction

The field of nonlinear optical (NLO) materials based on polymers has been a target of intensive research activity during the past decades. Polymeric materials present a combination of the important characteristics such as the mechanical strength, processability, environmental stability, and large damage threshold. To date, the molecular basis for the NLO properties is now well established, and the ease with which various polymers can be synthesized and chemically modified through rational design has led to the development of various systems to meet the optical characteristics required for fabrication of integrated optical devices.<sup>1</sup>

Although several rigid chain polymer systems have been reported, there have been quite a few systematic examinations for the rigid chain polymers with flexibly attached NLO chromophores.<sup>2,3</sup> Recent studies on the thermotropic liquid crystalline phase behaviors of rigid rod polymers indicated that a combination of aliphatic flexible side groups and rigid backbone polymers such as wholly aromatic polyesters or polyamides with flexible alkyl side groups give rise to layered crystalline, liquid crystalline, and isotropic structures depending on the temperature.<sup>4,5</sup> In view of the intrinsic easy response of the liquid crystalline phases to external fields, we have directed our efforts toward the development of wholly aromatic polymers with side group NLO chromophores. The NLO materials investigated here are a series of rigid rod polymers containing chromophores, *N*-(4-nitrophenyl)-L-prolinol (NPPOH), in the side group. To obtain polymers that melt and are soluble, the NLO chromophores were incorporated into the main chain through flexible methylene spacers. Interestingly, it was found that the studied polymers are not liquid crystalline, but their thin films form nanoscale domain structures when exposed to the poling dc electric field.<sup>6</sup> These

materials also exhibited the greatly enhanced second harmonic generation (SHG) intensity compared to the estimated value from the oriented gas model and unusual poling behaviors.<sup>7</sup> Furthermore, the time dependence measurements of the SHG intensity showed that a spontaneous dipole alignment occurred when the poled film was simply heated to near  $T_g$  of the polymer or swelled in a solvent like methanol.<sup>8</sup>

In this report, we extend our study to investigate nonlinear optical properties of a series of aromatic polyesters with different alkyl tether length. After briefly describing the domain structures observed by atomic force microscopy (AFM), we examine the refractive indices of the polymers measured by waveguiding techniques and then the results on the p–p and s–p polarized SHG measurements. In the last section, the unusually low values of the tensor ratios so determined are discussed in terms of the morphological specificity of the thin films for the present polymer systems.

## Experimental Section

**Materials and Thin-Film Preparation.** The polymers were prepared by the solution condensation of 2,5-disubstituted terephthalic acid with hydroquinone. The details on the syntheses and characterization of NPP-functionalized monomer, 2,5-di-[*N*-(4-nitrophenyl)-L-prolinoxy]terephthalic acids and the corresponding polymers were given elsewhere.<sup>7</sup> The inherent viscosity, measured at a concentration of 0.1 g/dL in tetrachloroethane (TCE), and glass transition temperature ( $T_g$ ) are listed in Table 1.

Polymer films for optical measurements were prepared by dissolution of the polymers (ca. 70 mg/mL) in tetrachloroethane, followed by filtration through a 0.45  $\mu$ m syringe filter. The solutions were then spin-coated on a glass slide with spinning rate in the range 2000–4000 rpm. After spinning, the sample films were heated under vacuum at 60 °C for several days. The thickness of the films was measured by an Alpha-step 100 profilometer and a spectroscopic ellipsometry technique. The transverse electric (TE) and transverse magnetic (TM) refractive indices of the films were determined by the *m*-line method in a slab waveguide configuration with a prism coupler (Scholt SFS01 prism,  $n = 1.9299$  at 632.8 nm).

<sup>†</sup> Department of Applied Chemistry.

<sup>‡</sup> Department of Physics.

\* Corresponding author.

**Table 1. Values of  $T_g$ 's and Inherent Viscosities for Studied Polymers P-4 to P-10**

	P-4	P-5	P-6	P-7	P-8	P-9	P-10
$\eta_{inh}$	0.38	0.89	0.29	0.67	0.20	0.10	0.33
$T_g$ (°C)	68	63	56	50	41	34	30

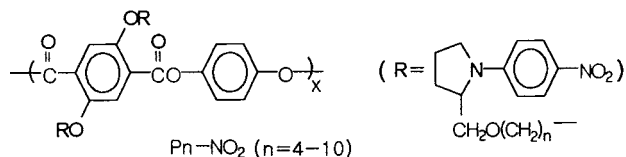
**AFM Measurements.** All AFM images were recorded with a Park Science Instrument Autoprobe LS, operated in a contact mode which measures topography by sliding the probe tip across the sample surface in air. The AFM images were represented here as three-dimensional figures, and the Z scale was magnified in order to enhance the surface morphology.

**Corona Poling and Second Harmonic Generation.** To induce noncentrosymmetric polar order, the spin-coated films were corona-poled under a voltage of 5 kV in air. The corona discharge was produced by holding at a given voltage a 25  $\mu$ m tungsten wire positioned parallel to the polymer surface at a distance of 1.0 cm from the surface. For purposes of comparison, the poling process was standardized to conditions to yield maximum SHG intensity at a given temperature (10 K above  $T_g$  of the polymers) and poling voltage. Particularities concerning the poling process have recently been reported in detail elsewhere.<sup>6,7</sup> Suffice it to say that a positive voltage should be applied to the wire electrode to obtain the orientation of chromophores.

Second harmonic generation measurements were made using a conventional Maker fringe technique. A mode-locked Q switched Nd:YAG laser ( $\lambda = 1.064 \mu$ m) with pulse width of <10 ns and repetition rate of 10 Hz was used as the fundamental light source. The details on the setup were described elsewhere.<sup>6</sup> When corona poling was used in situ, the film surface was oriented at an angle (usually 45°) relative to the incident laser beam. A Y-cut quartz single crystal (1 mm thick) was used as reference for the calibration of the SHG intensity. Two polarization modes were used. The first involved the p-p fundamental harmonic beam polarization configuration, and the second was in the s-p polarization configuration.

## Results and Discussion

A systematic study has been undertaken to characterize the linear and nonlinear optical properties for a series of wholly aromatic polyesters with different alkyl tether length. The samples are designated with the notation P-*n*, where *n* refers to the number of methylene spacers and varies from 4 to 10 (see the following repeat structure of the polymer).



**Domain Structure.** In the first place, we report our observations on the domain structure since we have observed it for the first time and considered it important to understand the following NLO results. Figure 1 shows AFM scans of the spin-coated film before and after poling for polymers P-4 to P-10. Figure 1a shows an AFM scan, typical for the spin-coated samples for the polymers before poling. The surface is extremely flat and clean. The root-mean-square roughness value obtained from the AFM software was 2.5 Å. However, this excellent quality film was dramatically changed after poling, resulting in numerous hills and valleys in the surface structure, which were aligned in the poling direction. The surface topographies shown in Figure 1 were characteristic of all samples although their statistical data were different in each of the samples and poling conditions studied. Figure 1c,d indicated that

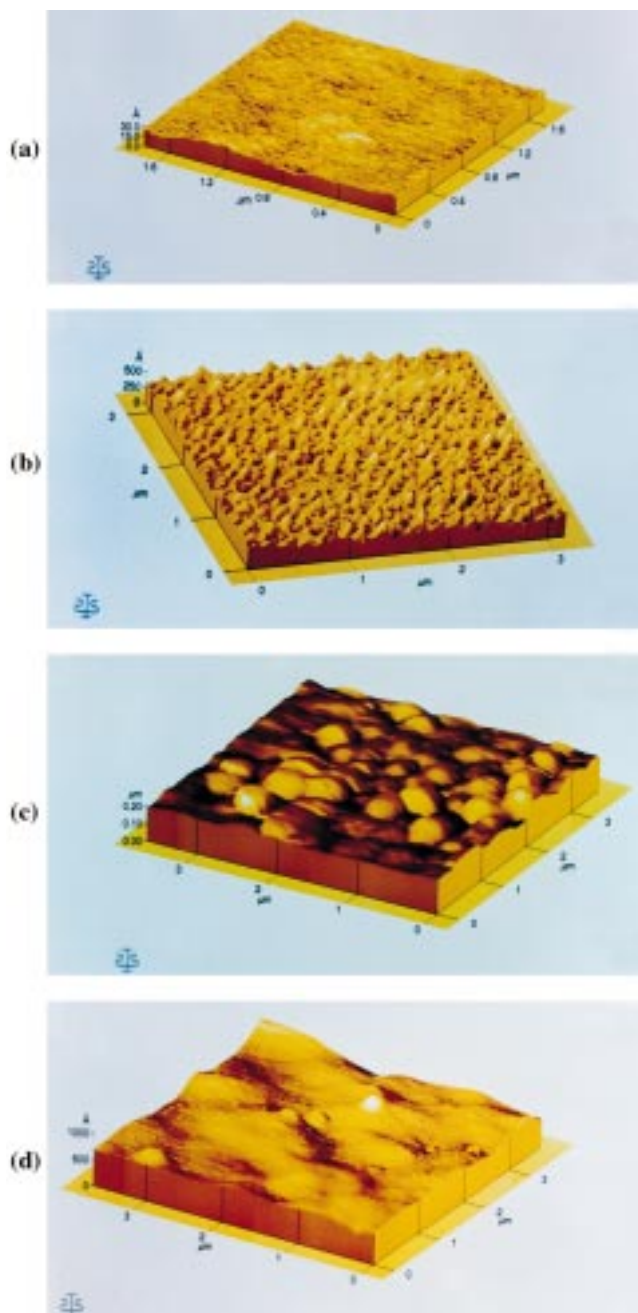


**Figure 1.** AFM images as spin-coated (a) followed by corona-poled (b) for a polymer film of P-4. The AFM scans (c) and (d) were taken for corona-poled films of P-6 and P-10, respectively.

poled polymer films showed a less well developed surface structure as *n* increased, a result caused by the reduced coupling effect of the side group with the backbone. A polymer that possesses a longer spacer unit between the NLO side group and the backbone gives a material in which NLO side groups are more mobile than when a shorter group is present.

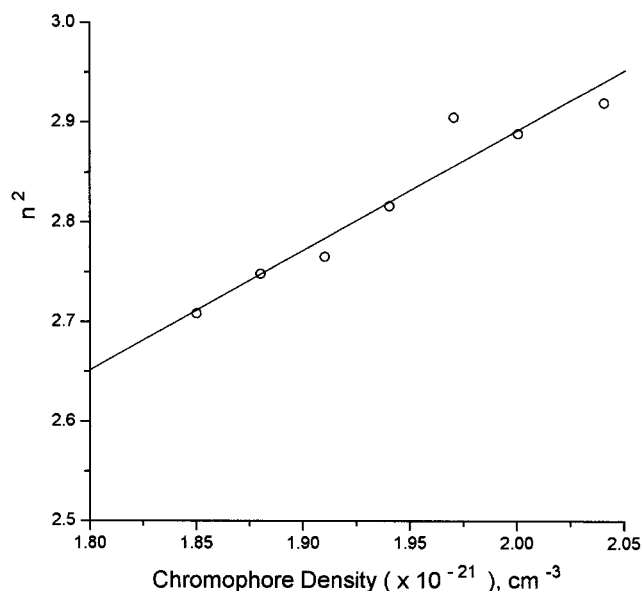
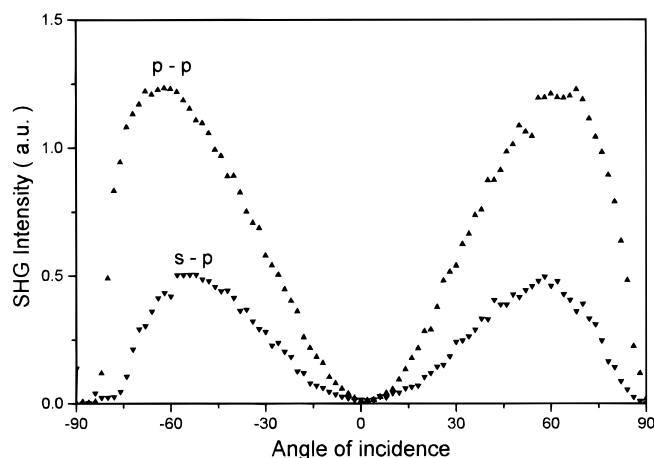
**Refractive Indices.** The refractive indices were measured using a prism coupler at 632.8 nm for the polymers, and the results are listed in Table 2. Measurements corresponding to the refractive indices of the TM and TE modes displayed considerable anisotropy for the films as spin-coated and poled. The birefringences defined as  $\Delta n = n_{TM} - n_{TE}$  are higher for the polymers with shorter alkyl tether length, indicating polymer molecules with shorter side groups are more highly oriented during spin-coating. Moreover, the negative

**Table 2. Results of Refractive Index Measurement**

polymer ( <i>n</i> )	TM mode		TE mode	
	before	after	before	after
4	1.7023	1.7537	1.7107	1.6863
5	1.6986	1.7324	1.7041	1.6833
6	1.7020	1.7049	1.7093	1.7043
7	1.6656	1.6983	1.6917	1.6682
8	1.6620	1.6883	1.6649	1.6504
9	1.6565	1.6767	1.6598	1.6483
10	1.6464	1.6613	1.6499	1.6380

birefringence reflects that the optically anisotropic groups were largely contained in the film plane. The origin of this birefringence is discussed below in terms of the rigid backbone chain.

Thin films were prepared by spin-coating TCE solution of the polymer on cleaned microscope glass slides. The spin-coating process leads to planar orientation of rigid backbone chains by flow-induced planar stacking of the backbone segments, and the side chromophores are probably tilted with respect to the main chain layers in order to decrease the distance between neighboring side groups.<sup>2</sup> The orientation of polymeric chains during film preparation is not uncommon. According to Prest and Luca,<sup>10</sup> the flexible polymers such as polystyrene and polycarbonate were preferentially aligned in the film plane during the spin-coating process, and they interpreted this alignment to be the result of the competition between the rapidly increasing relaxation times of the concentrating solution and the time scales of the collapse of the sample and molecular dimension. When the prepared films are poled, the chromophores are oriented in the direction perpendicular to the plane of the film, and hence the refractive indices of the TM mode increase whereas those of the TE mode decrease. Since the optical properties of these polymers are dominated by the anisotropic polarizability of the pendant chromophore, we examined a relation between the index of refraction and the number density of the chromophore. The density of the chromophore was calculated using the fractional mass of the chromophore in the polyester matrix. To a first approximation, the index of refraction in an independent response model is given by  $n^2 - 1 = \sum (N/V) \alpha_i$ .<sup>11</sup> The square of the index of refraction is thus linearly related to the polarizability  $\alpha_i$  per unit volume  $V_i$ . Figure 2 shows the square of the average index of refraction  $\langle n \rangle = 1/3(n_{TM} + 2n_{TE})$  as a function of chromophore density. The number density was calculated using the fractional mass of the chromophore, 46% in the polyester matrix, and an assumed density of 1.4 g/cm<sup>3</sup>.<sup>4</sup> Despite the scatter in the data, the observed linear relation implies that the molecular polarizability of the chromophores was not altered significantly by chromophore–chromophore pairing interaction even when the flexibility of the side groups increased with the number of methylene spacers. However, the dipole interactions in the surface domain cannot be ruled out in the interpretation since the requirement of at least three waveguide modes mandated a larger sample thickness, and the thin domain layer of highly oriented chromophores would contribute much less to the measured index of refraction. We believe that the observed conical shape of domains might be indicative of a slipped-deck-of-cards stacking arrangement of the chromophores, where the donor substituent of one molecular unit is in close spatial proximity to the acceptor substituent of the nearest neighbor.

**Figure 2.** Square of the average index of refraction as a function of chromophore density. The solid curve is a linear least-squares best fit to the data.**Figure 3.** SHG intensities (a) p-p-polarized (open circle) and (b) s-p-polarized (up triangle) for a 0.57  $\mu\text{m}$  sample of P-6 as a function of fundamental beam incident angle.**Table 3. Results of SHG (au) and Thickness Measurements for Studied Polymer Films**

polymer ( <i>n</i> )	$I_{p-p}$	$I_{s-p}$	$(I_{p-p}/I_{s-p})^{1/2}$	thickness ( $\mu\text{m}$ )	thickness-normalized $I_{shg}$
4	0.92	0.42	1.48	0.43	2.36
5	0.52	0.23	1.50	0.37	1.95
6	0.24	0.09	1.63	0.57	1.74
8	1.56	0.35	2.11	0.78	1.59
10	0.52	0.14	1.93	0.55	1.32

**Nonlinear Optical Properties.** The SHG intensity of the films was measured using either p (parallel polarized) or s (horizontal polarized) excitation and p detection. Figure 3 shows the typical Maker fringes for a polymer with tether length  $n = 6$ . The measured intensity values quoted in Table 3 are relative to peak-to-peak intensities measured on a crystal sample of quartz. Note also that care was taken to choose the SHG signal monitoring points on the films for the purpose of measurement reproducibility because the corona poling resulted in considerable variations in the SHG intensity from different locations on the films.

To determine the second-order NLO susceptibility  $d_{33}$ , we have tried to first fit the data by fixing the thickness



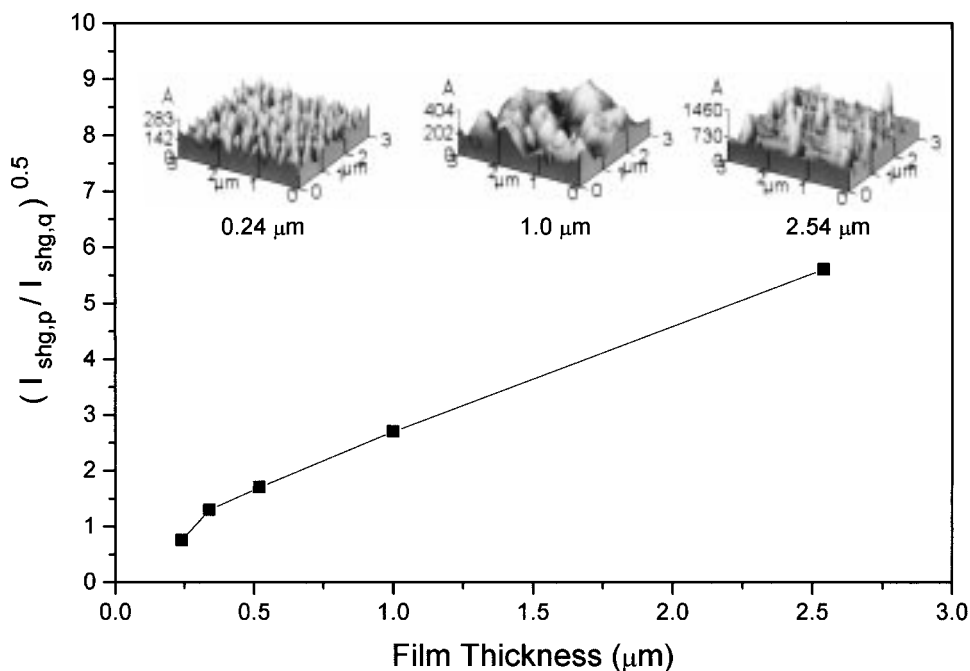


**Figure 4.** Square root of the SHG intensities as a function of the film thickness for polymer P-4. The insets are the AFM images for the polymer films with thicknesses of 0.24, 1.0, and 2.54  $\mu\text{m}$ .

at the measured sample thickness and varying only  $d_{33}$ . Apparently, this did not work. The experimental data were systematically deviated from the theoretical curves by Jerphagnon and Kurtz.<sup>12</sup> However, including the thickness as fit parameters usually did improve the fit significantly, and the fitted thickness was revealed to be much smaller than the measured film thickness. It is not clear, at the present time, whether this fitting failure is an artifact, but it could be speculated that the discrepancy between the two thicknesses is associated with the domain structure formed on the surface of the films. During poling, the chromophores in the surface layer will be oriented to a larger degree than those in the interior as they are less restricted and will thereby contribute to a larger extent to the overall SHG signal. Once the domain structure is formed, the chromophores in the domain would not readily reorient even though the surface charge dissipates. Figure 4 shows the AFM images and the square root of SHG intensities against the film thickness for the polymer P-4. As the film thickness increases, the surface morphology becomes much rougher as a consequence of the larger size of the structure, and the SHG signal does not increase up to the level expected from the theoretical  $I^2$  dependence even when the film thickness is far smaller than the coherence length of about 2.1  $\mu\text{m}$ . This decrease in the  $d$  value with the film thickness confirms that the relative fraction of the domain layer decreases as the film thickness increases. An attempt to measure the domain thickness is in progress, and the fitting results will be reported later.

Since quantitative information on  $d$  values could not be deduced, the thickness normalized SHG intensities were compared for the polymers with different tether length. It should be noted that the  $d$  values or the thickness normalized SHG intensities presented here should be considered to be approximate since we have neglected the depth dependence of orientation. When the film thickness is much smaller than the coherence length, the SHG signal shows the  $I^2$  dependence, when  $I$  is the thickness of the film. The second-order nonlinear

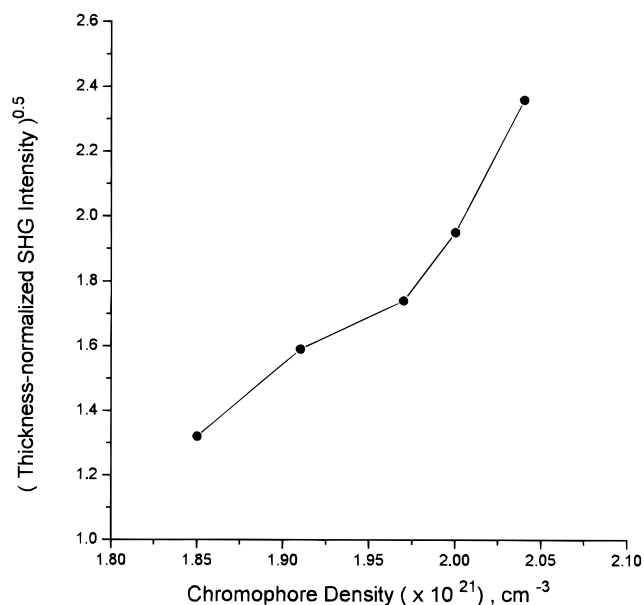


**Figure 5.** Thickness-normalized SHG intensity as a function of chromophore density.

susceptibility coefficient  $d$  then depends on  $I$  since the measured SHG intensity  $I_{\text{shg}}$  is related to  $d^2$ .<sup>13</sup> Accordingly, the  $I_{\text{shg}}^{1/2}$  normalized to unit thickness or  $I_{\text{shg}}^{1/2}/I$  can be used to compare the SHG coefficient for the different polymers. Figure 5 shows such a plot of the data shown in Table 3. It can be seen that even for small ranges of the chromophores density, significant deviation from the linear relationship between the SHG coefficient and the chromophore density was observed. Interestingly, the kind of departure from the direct proportionality is opposite to the deviations that are usually encountered when the chromophores pair due to dipole-dipole interaction, thereby reducing the SHG response. We believe that the departure from the linearity results from the domain structures, in which the chromophores are probably arranged like a slipped-deck-of-cards as mentioned previously. We confirmed

the orientationally correlated structure by the red shift in the UV absorption spectra, and the order parameter was calculated to be 0.58 for a poled film of P-4, which was the highest among the measured values for poled polymers with different tether lengths. Note that the experimental point at the lowest density was lower than the expected asymptote. This may be the result of fast relaxation occurring during the SHG measurements since the  $T_g$  of this polymer (30 °C) is near a measuring ambient temperature.

**Tensor Ratio.** The poled polymer films have a  $\infty mm$  symmetry with two tensor components of the second-order NLO susceptibility coefficients,  $d_{33}$  and  $d_{13}$ . Various orientation models have been proposed to describe the orientation of NLO chromophores for the poled polymers. The isotropic model predicts that the ratio of tensor components 33 and 13 is 3 for a purely electronic response.<sup>11</sup> We have calculated such tensor ratios from the square root of the corresponding SHG peak intensities.<sup>14</sup> The ratios were revealed to be much smaller than 3 for all the polymers (Table 3), indicating that the NLO chromophores are not Boltzmann-distributed in the poling field and do not obey Langevin formalism. A tensor ratio less than 3 is quite surprising since the relationship  $d_{33}/d_{31} > 3$  has been observed for many polymers, particularly for the polymers with a restricted rotational freedom of chromophore molecules, and theoretically it varies between 3 in isotropic systems and  $\infty$  for a perfect ordering. For example, tensor ratios in the 8–15 range were reported in the literature for liquid crystalline polymers,<sup>15</sup> and a ratio of 6 was observed for the poly(methyl methacrylates) with side group chromophores.<sup>16</sup> Considering the spin-coating process tends to induce planar orientations of rigid backbone chains for the present system, the easy plane of rotation should be in the plane of the film. So, it can be difficult to orient the chromophores by an applied electric field, and this is reflected during poling by the formation of domain structures described above. Such a restricted motion of the chromophore should have led to the values of the tensor ratios greater than 3.

The chromophores strained during poling may provide a possible explanation of this discrepancy. The large values of the  $d_{13}$  component relative to the  $d_{33}$  component reflect the depletion of the orientation distribution function perpendicular to the film plane. This suggests that the chromophores highly oriented perpendicularly to the film plane are localized in the surface domain region, and the rest of the chromophores contribute little to the inflation of the tensor ratio. Further, the chromophores in the interior would be strained due to the rigid upper layer while possessing the asymmetry necessary to exhibit second-order NLO processes and thereby contributing to a larger extent to the  $d_{13}$  component. Kuzyk and co-workers<sup>14</sup> predicted the ratio of the tensor components for polymer films poled under uniaxial stress based on a nonpolar potential, and the measured distribution function was consistent with the expected compression of molecules oriented in the film plane normal to the direction of the applied uniaxial stress. They observed that the range in the tensor ratio was found to be in a region of 3 with a film under no stress and 1.4 with a film under moderate stress ( $\sim 370$  MPa). Our measured tensor ratios lay in the region of theoretically predicted values for poled films under moderate stress, and this result seems to be reasonable considering the observed changes in the film thickness

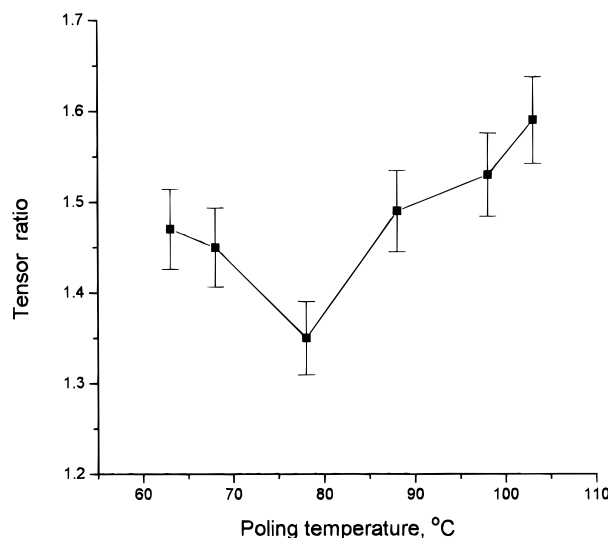


**Figure 6.** Tensor ratio as a function of poling temperature for P-4.

during poling. We have observed using in situ spectroscopic ellipsometry that the thickness of the film increased by 7.6–13.1% of its initial thickness depending on the thickness of the films when poled. The increase in physical thickness may arise from various mechanisms: piezoelectric and higher-order effects such as electrostriction and the Kerr effect.<sup>17</sup> The electrostriction mechanism is expected to give a dominant effect on the thickness change for the present system due to the large SHG intensity values.<sup>18</sup> The poling field gradients in the film result in a net force on the dipole moments of the chromophores, which results in an increase in thickness due to the layerlike structure of the film. However, the chromophore molecules in the interior, whose direction of the dipolar orientation is not parallel to the direction of the applied poling electric field, would experience a compressive force owing to the rigid neighboring layer. As the temperature approaches the poling temperature near  $T_g$  of the polymer, such a compressive stress is released, in part, by the change of the physical dimension of the sample; the residual force develops internal stress as the chromophores in the interior are more restricted, and the value of this stress may be on the order of hundreds of MPa. The thickness change and the observed birefringence are consistent with this picture.

Figure 6 shows the tensor ratio against the poling temperature for polymer P-4. The measured tensor ratio (estimated precision 3%) changed significantly as the poling temperature varied. The effect of temperature on the tensor ratio seems complicated. The measured SHG intensity increased with the poling temperature in the studied temperature range between 63 and 103 °C for a voltage of 5 kV. However, it showed a maximum when the poling voltage was lowered at 3 kV. The alignment of chromophore dipoles involves both interaction energy between the poling electric field and the dipole and thermal energy. The observed maximum may be the result of chromophore alignments enhanced by increasing molecular mobility at lower temperatures and by diminishing relative electric field drive with respect to the prevailing thermal energy as the temperature is elevated much above the glass transition. The tensor ratios in Figure 6 depend on the two SHG intensities of p–p and s–p configurations, and no definite mechanism can be offered to explain the results since very

little is known about the exact structure of these polymer films. At this stage, we can speculate that the stress due to electrostriction should be balanced by the elasticity of the polymer, and the electrostriction effect should decrease as the poling temperature increases since electric conductivity of the polymers increases drastically with the temperature above  $T_g$  of the polymer and current can flow through a film without developing a large voltage drop. On the other hand, if the poling temperature is too low, the viscosity of the polymer is too high for appreciable molecular movement so the tensor ratio cannot change continuously with decreasing temperature. Note that the results presented here are consistent with our observations on the domain formation, and they suggest that a thin skin region consisting of vertically oriented chromophores contributes to the measured p-p-polarized SHG intensity and an inner region with tilted chromophores contributes significantly to the measured s-p-polarized SHG intensity.

### Conclusion

We have presented the refractive indices and second-order NLO properties for the polymers in which the NLO chromophores are attached through different alkyl tether length in the side group. The measured refractive indices indicated considerable anisotropy for the polymer films as spin-coated and poled. The origin of this anisotropy was discussed in terms of the rigid character of the backbone chain. The thickness normalized SHG intensities were compared for the polymers with different tether lengths. Even for small ranges of the chromophore density studied, significant deviation from the linear relationship was observed between the SHG coefficient and the chromophore density. The departure from the linearity seemed to result from the domain structures, in which the chromophores may be orientationally correlated. The tensor ratios measured by the relative SHG intensity of either p or s excitation and p detection modes were found to be smaller than  $d_{33}/d_{13}$

= 3, the value predicted by an isotropic model. This deviation from Langevin formalism was discussed by the morphological features of these polymer films.

**Acknowledgment.** The authors gratefully acknowledge partial funding support from the Korea Science & Engineering Foundation (941-1100-011-2).

### References and Notes

- (1) See for example: Dalton, D. R.; Harper, A. W.; Ghosn, R.; Steier, W. H.; Ziari, M.; Fetterman, H.; Shi, Y.; Mustacich, R. V.; Jen, A. K.-Y.; Shea, K. J. *Chem. Mater.* **1995**, *7*, 1060.
- (2) Burland, D. M.; Miller, R. D.; Walsh, C. A. *Chem. Rev.* **1994**, *94*, 31. *Nonlinear Optics of Organic Molecules and Polymers*; Nalwa, H. S., Miyata, S., Eds.; CRC Press: New York, 1997.
- (3) Heldman, C.; Schulze, M.; Wegner, G. *Macromolecules* **1996**, *29*, 4686.
- (4) Heldman, C.; Neher, D.; Winkelhahn, H.-J.; Wegner, G. *Macromolecules* **1996**, *29*, 4697.
- (5) Ballauff, M. *Angew. Chem., Int. Ed. Engl.* **1989**, *28*, 253.
- (6) Damman, S. B.; Mercx, F. P. M. *J. Polym. Sci., Polym. Phys. Ed.* **1993**, *31*, 1759.
- (7) Lee, S. H.; Kang, Y. S.; Song, S. J. *Chem. Commun.* **1998**, 2513.
- (8) Lee, S. H.; Song, W. S.; Jung, M. J.; Jeon, I. C.; Ahn, B. G.; Song, S. J. *Bull. Korean Chem. Soc.* **1997**, *18*, 8.
- (9) Lee, S. H.; Kim, C. K.; Lee, M. W.; Won, Y. H., to be published.
- (10) Lee, S. H.; Lim, K. C.; Jeon, J. T.; Song, S. J. *Bull. Korean Chem. Soc.* **1996**, *17*, 11.
- (11) Prest, W. M.; Luca, D. J. *J. Appl. Phys.* **1980**, *51*, 5170.
- (12) Born, M.; Wolf, E. *Principles of Optics*; Pergamon: Oxford, 1980.
- (13) Jerphagnon, J.; Kurtz, S. K. *J. Appl. Phys.* **1970**, *41*, 1667.
- (14) Kurtz, S. K.; Perry, T. T. *J. Appl. Phys.* **1968**, *89*, 8798.
- (15) Kuzyk, M. G.; Singer, K. D.; Zahn, H. E.; King, L. A. *J. Opt. Soc. Am. B* **1989**, *6*, 742.
- (16) Gonin, D.; Guichard, B.; Noel, C.; Kajzar, F. In *Polymers and Other Advanced Materials: Merging Technologies and Business Opportunities*; Prasad, P. N., Eds.; Plenum Press: New York, 1995.
- (17) Herminghaus, S.; Barton, A. S.; Swalen, J. D. *J. Opt. Soc. Am. B* **1991**, *8*, 2311.
- (18) Morichere, D.; Dentan, V.; Kajzar, F.; Robin, P.; Levy, Y.; Dumont, M. *Opt. Commun.* **1989**, *74*, 69.
- (19) Norwood, R. A.; Kuzyk, M. G.; Keosian, R. A. *J. Appl. Phys.* **1994**, *75*, 1869.

MA9807421